Inorg. Chem. **2006**, *45*, 269–277

Mixed Guanidinato/Alkylimido/Azido Tungsten(VI) Complexes: Synthesis and Structural Characterization

Daniel Rische, Arne Baunemann, Manuela Winter, and Roland A. Fischer*

Lehrstuhl für anorganische Chemie II, Ruhr-Universität Bochum, NC 2, Universitätsstr. 150, 44801 Bochum, Germany

Received July 26, 2005

A series of structurally characterized new examples of pentacoordinated heteroleptic tungsten(VI)–guanidinates complexes are described. Starting out from $[WCl_2(N\textit{t}\text{-}Bu)_2py_2]$ (**1**) (py = pyridine) and the guanidinato transfer reagents (TMEDA)Li[$(N\textit{i}\text{-}Pr)_2CN\textit{i}\text{-}Pr_2$] (**2a**) (TMEDA = *N*,*N*,*N*′,*N*′-tetramethylethylendiamine) and $[Li(NC(NMe_2)_2)]_x$ (**2b**), the title compounds $[WCl(N\textit{t}\text{-}Bu)_2\{(N\textit{i}\text{-}Pr)_2CN\textit{i}\text{-}Pr_2\}]$ (**3**) and $[W(N\textit{t}\text{-}Bu)_2Cl\{NC(NMe_2)_2\}]_2$ (**6**) were selectively formed by the elimination of one mole equivalent of lithium chloride. The isopropyl-substituted guanidinato ligand $\{(N\textit{i}\text{-}Pr)_2CN\textit{i}\text{-}Pr_2\}$ of monomeric **3** is N^1,N^3-bonded to the tungsten center. The introduction of the sterically less-demanding tetramethyl guanidinato ligand $\{NC(NMe_2)_2\}$ expectedly leads to dimeric **6** exhibiting a planar W_2N_2 ring with the guanidinato group bridging the two tungsten centers via the deprotonated imino N-atom. The remaining chloro ligand of **3** is labile and can be substituted by sterically less-crowded groups such as dimethylamido or azido that yield the presumably monomeric compounds **4** and **5**, respectively. A similar treatment of **6** with sodium azide yields the dimeric azido derivative **7**. Reacting $[WCl_2(N\textit{t}\text{-}Bu)_2py_2]$ directly with an excess of sodium azide leads to the dimeric bis-azide species $[\{W(N\textit{t}\text{-}Bu)_2(N_3)(\mu^2\text{-}N_3)py\}_2]$. The new compounds were fully characterized by single-crystal X-ray diffractometry (except **2**, **4**, and **5**), NMR, IR, and mass-spectroscopy as well as elemental analysis. Compound **5**, $[W(N_3)(N\textit{t}\text{-}Bu)_2\{(N\textit{i}\text{-}Pr)_2CN\textit{i}\text{-}Pr_2\}]$, can be sublimed at 80 °C, 1 Pa.

Introduction

Since the first guanidinato complexes have been reported in 1970 by Lappert et al.,[1] guanidinato ligands, $\{NC(NR_2)_2^-\}$ and $\{(NR)_2C(NR_2)^-\}$, have been found to support all metal ions across the periodic table. These ligands bind to main-group metals[2−4] and transition metals[2,5,6] as well as to lanthanides.[2,7] The characteristic feature of all guanidinato complexes is a trigonal planar CN_3 unit substituted by organic groups being isoelectronic to the monoanionic hydrogen carbonato HCO_3^- ligand. The steric and electronic properties of the guanidinato group can be tuned by variation of the hydrocarbon residues, R. In the case of a planar CN_3 unit, all atoms are sp^2-hybridized, and thus, an overlap of all lone pairs at the nitrogen atoms is possible, which leads to very short C−N distances. This effect has been claimed as Y-aromaticity.[2] Guanidinato ligands are highly tunable, and the style of bonding to metal centers can vary considerably. The type I ligands, $\{NC(NR_2)_2^-\}$, are known to bind via the imino N-atom in an η^1 mode.[8] The type II congeners, $\{(NR)_2C(NR_2)^-\}$, bind in an η^2 fashion involving the N^1 and N^3 atoms, and the dialkylamido group of N^2 is not coordinated.[2−7] Type II represents the most common form of guanidinato ligands. There are also a few examples known where the guanidinate is bonded as a dianionic ligand;[2,9] as well, neutral, not deprotonated guanidines can bind as donor ligands.[2]

Over the last years, guanidinato ligands have gained considerable interest beyond fundamental structural coordination chemistry. Many guanidinato complexes have been identified as being excellent initiators or catalysts for electrophilic polymerization reactions, e.g., trimethylene

* Author to whom correspondence should be addressed. E-Mail: Roland.Fischer@rub.de.

(1) Chandra, G.; Jenkins A. D.; Lappert, M. F.; Srivastava, R. C. *J. Chem. Soc. A* **1970**, 2550.
(2) Bailey P. J.; Pace, S. *Coord. Chem. Rev.* **2001**, *214*, 91.
(3) Kenney, A. P.; Yap, G. P. A.; Richeson, D. S.; Barry, S. T. *Inorg. Chem.* **2005**, *44*, 2926.
(4) Chang, C.-C.; Hsiung, C.-S.; Su, H. L.; Srinivas, B.; Chiang, M. Y.; Lee, G.-L.; Wang, Y. *Organometallics* **1998**, *17*, 1585.
(5) Ong, T.-G.; Yap, G. P. A.; Richeson, D. S. *Chem. Commun.* **2003**, 2612.
(6) Zuckermann, R. L.; Bergman, R. G. *Organometallics* **2000**, *19*, 4795.
(7) Zhou, Y.; Yap, G. P. A.; Richeson, D. S. *Organometallics* **1998**, *17*, 4387.
(8) Kretschmer, W. P.; Dijkkuis, C.; Meetsma, A.; Hessen, B.; Teuben, J. H. *Chem. Commun.* **2002**, 608.
(9) Tin, M. K. T.; Yap, G. P. A.; Richeson, D. S. *Inorg. Chem.* **1998**, *37*, 6728.

10.1021/ic0512431 CCC: $33.50 © 2006 American Chemical Society
Published on Web 12/07/2005

carbonate and its copolymerization with ϵ-caprolactone[10] (which is initiated by an ytterbium guanidinate), the polymerization of lactide[11] (catalyzed by a homoleptic zinc guanidinate), the polymerization of α-olefins (which is catalyzed by a zirconium guanidinato complex[11]), or the polymerization of styrene[12] (which can be initiated by guanidinato complexes of neodymium or ytterbium). Thus, the chemistry of guanidinato complexes appears to be quite promising, particularly looking at novel types of tailored homogeneous catalysts for various reactions. Even more recently, guanidinato complexes of the early transition metals Ti and Ta have been studied as potential precursors for the growth of the respective metal nitride and/or carbonitride phases.[13,14] These nitride materials are interesting as both electronically insulating as well as conductive diffusion barriers on silicon in copper metallization of microelectronic circuits, enhancing the lifetime of the contacts. Similarly, various phases of tungsten nitride and carbonitride have been discussed as alternative diffusion barriers for similar purposes.[15−19] We have been attracted to the coordination chemistry of guanidinato complexes for the above two reasons. Recently we reported on the synthesis, structural chemistry, and characterization of novel guanidinato complexes of tantalum, including preliminary results of TaN thin film growth by metal organic chemical vapor deposition (MOCVD) using those compounds as novel precursors.[14] Below, we wish to present an account on our related work on the first structurally characterized guanidinato complexes of tungsten(VI) and some derivatives containing a mixed-ligand all-nitrogen coordinated sphere around the W center composed of a combination of guanidinato, alkylimido, alkylamido, and/or azido groups.

Experimental Section

General Procedures. All Manipulations were carried out using standard Schlenk and glovebox techniques. Hexane and toluene were dried over Al_2O_3 columns under Ar (99.99) using an automatic solvent purification system (M. Braun) directly connected to a glovebox (H_2O below 1 ppm, Karl Fischer). Pyridine was dried over Na/benzophenone, and TMEDA was dried over CaH_2. Both solvents were distilled prior to use. *N*,*N*′-Diisopropylcarbodiimide (98% purity) was purchased from Acros, and *n*-butyllithium (15 wt % solution in *n*-hexane) and diisopropylamine (99% purity) were purchased from Merck. WCl_6 (99.99% purity) was supplied by H. C. Starck. *N*-*tert*-Butyltrimethylsilylamine (98% purity) was purchased from Aldrich. 1,1,3,3-Tetramethylguanidine and sodium azide were obtained from Fluka. All starting compounds and reagents were used as received.

Synthesis of [WCl_2(N*t*-Bu)$_2$py$_2$] (1). A sample of WCl_6 (10 g, 25.6 mmol) was dissolved in 100 mL of toluene. A sample of HN(*t*-Bu)($SiMe_3$) (19.2 g, 0.1 mol) was added slowly, and the reaction mixture was allowed to stir overnight at room temperature. The resulting brown suspension was filtered through Celite, and the solvent and all volatile byproducts were removed by vacuum distillation at 25 °C. The residue was washed with 40 mL of *n*-hexane. The obtained yellow solid was allowed to settle, and the dark-brown washing solution was removed by filtration. The yellow intermediate was suspended in 50 mL of diethyl ether. After the addition of pyridine (20 mL), the reaction mixture immediately turned dark-green. After 1 h of stirring, the solvent was removed in vacuum to yield 7.55 g (54.2%) of a green microcrystalline powder. Pure **1** was obtained by recrystallization from toluene at room temperature after one week.

^{1}H NMR (C_6D_6, 298 K): δ 1.53 (s 18 H, N*t*-Bu); 6.51 (t, 4H, py); 6.84 (t, 2H, py), 9.09 (d, 4H, py).

^{13}C NMR (C_6D_6, 298 K): δ 31.5 (NC(**C**H_3)$_3$); 67.9 (N**C**(CH_3)$_3$); 123.3 (py); 136.9 (py); 152.1 (py).

Anal. Calcd for $WCl_2N_4C_{18}H_{28}$: C, 38.94; H, 5.08; N, 10.09. Found: C, 39.14; H, 5.06; N, 9.56.

Synthesis of [*i*-Pr$_2$NC(N*i*-Pr)$_2$Li(TMEDA)] (2a). A sample of 31.3 mL of butyllithium (15 wt %, *n*-hexane solution) was transferred into a Schlenk tube and cooled to −78 °C. Diisopropylamine (7 mL, 50 mmol) was added to the solution, which was then allowed to warm to room temperature. One equivalent of *N*,*N*′-diisopropylcarbodiimide (7.7 mL 50 mmol) was added, and the solution was stirred for 1 h at 25 °C. Subsequently, *N*,*N*,*N*′,*N*′-tetramethylethylendiamine (7.4 mL) was added to the yellow solution. After 1 h of stirring, the solvent was removed, and the product **2a** was obtained as a microcrystalline pale-yellow powder (17.02 g, 97.5%).

^{1}H NMR (C_6D_6, 298 K): δ 1.23 (d, 12H, CN(CH**Me**$_2$)$_2$); 1.38 (d, 12 H, C(NCH**Me**$_2$)$_2$), 1.88 (s, 4H, C**H**$_2$NMe$_2$), 2.02 (s, 12 H CH_2N**Me**$_2$), 3.59 (sept, 2H, CN(C**H**Me$_2$)$_2$); 3.90 (sept, 2 H, C(NC**H**Me$_2$)$_2$).

^{13}C NMR (C_6D_6, 298 K): δ 24.1(**Me**$_2$CH); 28.3 (**Me**$_2$CH); 45.9 (CH_2N**Me**$_2$); 46.1 (Me$_2$**C**H); 48.1 (Me$_2$**C**H); 56.7 (**C**H_2NMe$_2$); 164.6 (**C**N_3).

EI-MS [*m*/*z* (%)]: 227 (65) [(N*i*-Pr)$_2$CN*i*-Pr$_2$) + H]; 212 (20) [(N*i*-Pr)$_2$CN*i*-Pr$_2$) + H − Me]; 184 (52) [(N*i*-Pr)$_2$CN*i*-Pr) + H − *i*-Pr]; 127 (12) [(N*i*-Pr)$_2$C + H]; 116 (6) [TMEDA]; 113 (4) [*i*-Pr$_2$NC + H]; 100 (19) [*i*-Pr$_2$N]; 85 (30) [*i*-Pr$_2$N − Me]; 69 (16) [*i*-PrNC]; 58 (100) [*i*-PrN + H]; 43 (57) [*i*-Pr]; 27 (10) [HCN].

Anal. Calcd for $LiN_5C_{19}H_{40}$: C, 65.29; H, 12.69; N, 20.04; Li, 1.98. Found: C, 64.69; H, 11.12; N, 19.96; Li, 2.3.

Synthesis of [W(N*t*-Bu)$_2$Cl((N*i*-Pr)$_2$CN*i*-Pr$_2$)] (3). Equimolar samples of **1** (2.53 g, 4.5 mmol) and **2a** (1.57 g, 4.5 mmol) were dissolved in 40 mL of *n*-hexane. During stirring the green solution for 1 day at 25 °C, the color gradually turns to black. After filtration, all volatile parts were removed by standard vacuum distillation at 25 °C. The black crude product was recrystallized from saturated *n*-hexane solution to yield pure **3** (1.76 g, 66.6%) in the form of pale-yellow crystals.

^{1}H NMR (C_6D_6, 298 K): δ 0.97 (d, 6H, CNCH**Me**$_2$); 0.98 (d, 6H, CNCH**Me**$_2$); 1.11 (d, 6H, WNCH**Me**$_2$); 1.47 (s, 18H, N*t*-Bu);

(10) Zhou, L.; Sun, H.; Chen, J. Yao, Y.; Shen, Q. *J. Polym. Sci., Part A: Polym. Chem.* **2005**, *43*, 1778.
(11) (a) Coles, M. P.; Hitchcock, P. B. *Eur. J. Inorg. Chem.* **2004**, 2662. (b) Duncan, A. P.; Mullins, S. M.; Arnold, J.; Bergman, R. G. *Organometallics* **2001**, *20*, 1808. (c) Bazinet, P.; Wood, D.; Yap, G. P. A.; Richeson, D. S. *Inorg. Chem.* **2003**, *42*, 6225.
(12) Luo, Y.; Yao, Y.; Shen, Q. *Macromolecules* **2002**, *35*, 8670.
(13) Carmalt, C. J.; Newport, A. C.; O'Neill, S. A.; Parkin, I. P.; White, A. J. P.; Williams, D. J. *Inorg. Chem.* **2005**, *44*, 615.
(14) Baunemann, A.; Rische, D.; Milanov, A.; Gemel, C.; Fischer, R. A. *Dalton Trans.* **2005**, 3051.
(15) Crane, E. L.; Chiu, H.-T.; Nuzzo, R. G. *J. Phys. Chem. B* **2001**, *105*, 3549.
(16) Bchir, O. J.; Green, K. M.; Ajmera, H. M.; Zapp, E. A.; Anderson, T. J.; Brooks, B. C.; Reitfort, L. L.; Powell, D. H.; Abboud, K. A.; McElwee-White, L. *J. Am. Chem. Soc.* **2005**, *127*, 7825.
(17) Becker, J. S.; Suh, S. Wang, S. Gordon, R. G. *Chem. Mater.* **2003**, *15*, 2969.
(18) Dezelah, C. L.; El-Kadri, O. M.; Heeg, M. J.; Winter, C. H. *J. Mater. Chem.* **2004**, *14*, 3167.
(19) Bchir, O. J.; Green, K. M.; Hlad, M. S.; Anderson, T. J.; Brooks, B. C.; Wilder, C. B.; Powell, D. H.; McElwee-White, L. *J. Organomet. Chem.* **2003**, *684*, 338.

1.54 (d, 6H, WNCH**Me**$_2$); 3.17 (sept, 2H, CNC**H**Me$_2$); 4.08 (sept, 1H, WNC**H**Me$_2$); 4.15 (sept, 1H, WNC**H**Me$_2$).

^{13}C NMR (C_6D_6, 298 K): δ 22.6 (**Me**$_2$CH); 22.7 (**Me**$_2$CH); 24.3 (**Me**$_2$CH); 24.5 (**Me**$_2$CH); 32.6 (NC(**C**H$_3$)$_3$); 45.3 (Me$_2$**C**H); 47.8 (Me$_2$**C**H); 48.7 (Me$_2$**C**H); 67.4 (N**C**(CH$_3$)$_3$); 168.7 (**C**N$_3$).

EI-MS [*m*/*z* (%)]: 587 (8) [M$^+$]; 572 (8) [M$^+$ − Me]; 530 (4) [M$^+$ − *t*-Bu]; 473 (4) [M$^+$ − 2*t*-Bu]; 446 (18) [M$^+$ − 2N*t*-Bu]; 331 (4) [((*i*-PrN)$_2$ − W − Cl) − 2H]; 291 (10) [*t*-BuNH − W − Cl]; 226 (56) [(N*i*-Pr)$_2$CN*i*-Pr$_2$)]; 184 (68) [(N*i*-Pr)$_2$CN*i*-Pr) + H-*i*-Pr]; 169 (38) [(N*i*-Pr)$_2$CN*i*-Pr) − N*i*-Pr]; 127 (25) [(N*i*-Pr)$_2$C + H]; 113 (6) [*i*-Pr$_2$NC + H]; 100 (24) [*i*-Pr$_2$N]; 85 (40) [*i*-Pr$_2$N − Me]; 69 (24) [*i*-PrNC]; 58 (35) [*i*-PrN + H]; 43 (100) [*i*-Pr].

Anal. Calcd for WClN$_5$C$_{21}$H$_{46}$: C, 43.42; H, 6.76; N, 12.05. Found: C, 43.15; H, 7.55; N, 11.97.

Synthesis of [W(N*t*-Bu)$_2$NMe$_2$((N*i*-Pr)$_2$CN*i*-Pr$_2$)] (4). Equimolar samples of **3** (1.66 g, 2.7 mmol) and LiNMe$_2$ (0.14 g, 2.7 mmol) were placed in a Schlenk tube, and 40 mL of diethyl ether was added. After stirring the mixture at room temperature overnight, filtration, and removal of the solvent in vacuo, the analytically almost pure product was obtained as a yellow, viscous oil. Further attempts of purification by crystallization at low temperature and by distillation failed. Yield: 0.80 g (49.7%).

^{1}H NMR (C_6D_6, 298 K): δ 1.05 (d, 12H CNCH**Me**$_2$); 1.26 (d, 12H, WNCH**Me**$_2$); 1.48 (s, 18H, N*t*-Bu); 3.25 (sept, 2H, CNC**H**Me$_2$); 3.51 (s, 6H, N**Me**$_2$); 4.02 (sept, 2H, WNC**H**Me$_2$).

^{13}C NMR (C_6D_6, 298 K): δ 22.9 (**Me**$_2$CH); 24.9 (**Me**$_2$CH); 34.3 (NC(**C**H$_3$)$_3$); 48.4 (Me$_2$**C**H); 55.4 (Me$_2$**C**H); 66.6 (N**C**(CH$_3$)$_3$); 168.6 (**C**N$_3$).

EI-MS [*m*/*z* (%)]: 596 (1) [M$^+$]; 553 (4) [M$^+$ − *i*-Pr]; 508 (5) [M$^+$ − N*t*-Bu − Me]; 454 (5) [M$^+$ − 2N*t*-Bu]; 427 (1.5) [W(N*t*-Bu)$_2$NMe$_2$((N*i*-Pr)CN*i*-Pr)]; 371 (1.5) [W(N*t*-Bu)$_2$NMe$_2$ + H]; 300 (2,5) [W(N*t*-Bu)NMe$_2$]; 226 (30), [(N*i*-Pr)$_2$CN*i*-Pr$_2$]; 184 (16) [((N*i*-Pr)$_2$CN*i*-Pr$_2$) − *i*-Pr]; 169 (8) [((N*i*-Pr)$_2$CN*i*-Pr$_2$) − N*i*-Pr]; 127 (10) [C(N*i*-Pr)$_2$]; 100 (11) [N*i*-Pr$_2$]; 85 (30) [(N*i*-Pr$_2$) − Me]; 69 (19) [*i*-PrNC]; 58 (100) [*i*-PrN + H]; 43 (55) [*i*-Pr]; 28 (16) [H$_2$CN].

Anal. Calcd for WN$_6$C$_{23}$H$_{52}$: C, 46.31; H, 8.72; N, 14.09. Found: C, 45.34; H, 9.04; N, 13.37.

Synthesis of [W(N*t*-Bu)$_2$(N$_3$)((N*i*-Pr)$_2$CN*i*-Pr$_2$)] (5). A sample of **3** (1.0 g, 1.7 mmol) was treated with an excess of dry, finely powdered sodium azide (0.4 g, 6.1 mmol) in a mixture of toluene (40 mL) and THF (5 mL) in a Schlenk tube at reflux over 4 days. The formed NaCl and excess NaN_3 were removed by filtration, and the solvent was stripped in vacuo. The residue was dissolved in *n*-hexane and filtrated from insoluble byproducts. Stripping the solvent again left a yellow oily substance. The crude product was short-path distilled at 10^{-2} Torr (1 Pa) and 80 °C to give a yellow solid, which sublimes unchanged at the same conditions. Crystallization from toluene at −30 °C failed to give single crystals suitable for X-ray structural characterization. Yield: 0.65 g (64.4%).

^{1}H NMR (C_6D_6, 298 K): δ 0.92 (d, 6H, CNCH**Me**$_2$); 0.93 (d, 6H, CNCH**Me**$_2$); 1.06 (d, 6H, WNCH**Me**$_2$); 1.39 (d, 6H, WNCH**Me**$_2$); 1.46 (s, 18H, N*t*-Bu); 3.11 (sept, 2H, CNC**H**Me$_2$); 4.01 (sept, 2H, WNC**H**Me$_2$).

^{13}C NMR (C_6D_6, 298 K): δ 22.5 (**Me**$_2$CH); 22.6 (**Me**$_2$CH); 24.3 (**Me**$_2$CH); 24.4 (**Me**$_2$CH); 33.3 (NC(**C**H$_3$)$_3$); 45.2 (Me$_2$**C**H); 47.1 (Me$_2$**C**H); 48.7 (Me$_2$**C**H); 67.9 (N**C**(CH$_3$)$_3$); 168.5 (**C**N$_3$).

FT IR (dry film, cm^{-1}): 2086, vs (ν_{N-N}); 2970, vs (ν_{C-H}).

Anal. Calcd for WN$_8$C$_{21}$H$_{46}$: C, 42.42; H, 7.80; N, 18.84. Found: C, 41.82; H, 7.55; N, 18.50.

Synthesis of [W(N*t*-Bu)$_2$Cl{NC(NMe$_2$)$_2$}]$_2$ (6). A sample of 1.15 ml of 1,1,3,3-tetramethylguanidine (9 mmol) was dissolved in 40 mL of diethyl ether. A volume of 6 mL of butyllithium (15 wt %, solution in *n*-hexane, 9 mmol) was added at 0 °C, and the reaction mixture was allowed to stir for a period of 30 min. A white precipitate was formed, and the whole suspension was added to a solution of **1** (5.0 g) in toluene (30 mL). The mixture was refluxed for 24 h. After filtration, the solvent was stripped, and the crude product was recrystallized from toluene to yield 2.95 g (68.9%) of a microcrystalline pale-yellow powder. Well-shaped single crystals of **6** were obtained by recrystallization from *n*-hexane at −30 °C over 1 day.

^{1}H NMR (C_7D_8, 223 K): δ 1.54 (s, 18H, N*t*-Bu); 2.39 (6H, N**Me**$_2$); 3.05 (6H, N**Me**$_2$).

^{13}C NMR (C_6D_6, 298 K): δ 33.1 (NC(**C**H$_3$)$_3$); 40.6 (broad, N**Me**$_2$); 66.8 (N**C**(CH$_3$)$_3$); 178.4 (**C**N$_3$).

EI-MS [*m*/*z* (%)]: 475 (1,6) [M$^+$/2]; 460 (8) [M$^+$/2 − Me]; 390 (1) [M$^+$/2 − Me − NtBu + H]; 334 (2,5) [M$^+$/2 − 2N*t*-Bu + H]; 318 [M$^+$/2 − 2N*t*-Bu − Me]; 291 (1,2) [*t*-BuNH − W−Cl]; 184 (20) [W$^+$]; 115 (48) [NH═C(NMe$_2$)$_2$]; 86 (16) [(Me$_2$N)$_2$C − Me]; 71 (95) [N*t*-Bu]; 58 (100) [*t*-Bu + H]; 44 (52) [NMe$_2$]; 27 (17) [HCN].

Anal. Calcd for W$_2$Cl$_2$N$_{10}$C$_{26}$H$_{60}$: C, 32.83; H, 6.36; N, 14.72. Found: C, 32.74; H, 6.36; N, 14.61.

Synthesis of [(W(N*t*-Bu)$_2$(N$_3$){NC(NMe$_2$)$_2$}]$_2$ (7). 6 (1.0 g, 1.05 mmol) was combined with dried and finely powdered NaN_3 (0.5 g, 7.6 mmol) in a Schlenk tube. Toluene (50 mL) and THF (5 mL) were added, and the mixture was refluxed for 1 day. The precipitated NaCl and excess NaN_3 were removed by filtration, and the solvent was stripped in vacuo at 25 °C. The crude product was recrystallized from toluene at −30 °C to give 0.86 g (84.4%) of yellow crystals.

^{1}H NMR (C_6D_6, 298 K): δ 1.46 (s, 18H, N*t*-Bu); 2.71 (s, 12H, N**Me**$_2$).

^{13}C NMR (C_6D_6, 298 K): δ 33.7 (NC(**C**H$_3$)$_3$); 40.2 (N**Me**$_2$); 67.3 (N**C**(CH$_3$)$_3$); 176.8 (**C**N$_3$).

FT IR (toluene solution, cm^{-1}): 2072, vs (ν_{N-N}).

Anal. Calcd for W$_2$N$_{16}$C$_{26}$H$_{60}$: C, 32.37; H, 6.33; N, 23.23. Found: C, 32.76; H, 6.68; N, 22.74.

Synthesis of [(W(N*t*-Bu)$_2$(N$_3$)(μ^2-N$_3$)py)]$_2$ (8). 1 (1.0 g, 1.8 mmol) was combined with dried and finely powdered NaN_3 (0.5 g, 7.6 mmol) in a Schlenk tube. Toluene (50 mL) and THF (5 mL) were added, and the mixture was heated to reflux for 1 day. The precipitated NaCl and excess NaN_3 were removed by filtration, and the solvent was stripped in vacuo at 25 °C. Crystals of **8** were obtained by diffusion crystallization at 25 °C, placing a layer of pentane over a concentrated toluene solution of the crude product. Yield: 0.38 g (43.1%).

^{1}H NMR (C_6D_6, 298 K): δ 1.41 (s 36 H, N*t*-Bu); 6.62 (t, 4H, py); 8.64 (t, 2H, py); 8.96 (d, 4H, py).

^{13}C NMR (C_6D_6, 298 K): δ 32.8 (NC(**C**H$_3$)$_3$); 68.3 (N**C**(CH$_3$)$_3$); 125.2 (py); 139.1 (py); 153.5 (py).

FT IR (toluene solution, cm^{-1}): 2082, vs (ν_{N-N}).

Anal. Calcd for W$_2$N$_{18}$C$_{26}$H$_{46}$: C, 31.91; H, 4.74; N, 25.77. Found: C, 31.24; H, 4.96; N, 24.24.

X-ray Single-Crystal Diffraction and Structure Determination of 1, 3, 6, 7, and 8. The X-ray single-crystal diffraction data accumulation of compounds **1**, **6**, **7**, and **8** were performed on an Oxford Excalibur 2 diffractometer. For the measurement of **3**, a Bruker SMART CCD 1000 diffractometer was used.All structures were solved by direct methods (SHELXL-97) and refined by a full-matrix least-squares method based on F^2 using SHELXL-97. The employed programs were SHELXS-97 and SHELXL-97. CCDC 291383 (**1**), CCDC 291384 (**3**), CCDC 291385 (**6**), CCDC 291386 (**7**), and CCDC 291387 (**8**), contain the supplementary crystallographic data for these structure determinations. These data can be obtain free of charge via http://www.ccdc.cam.ac.uk/conts/retrieving.html.

Scheme 1

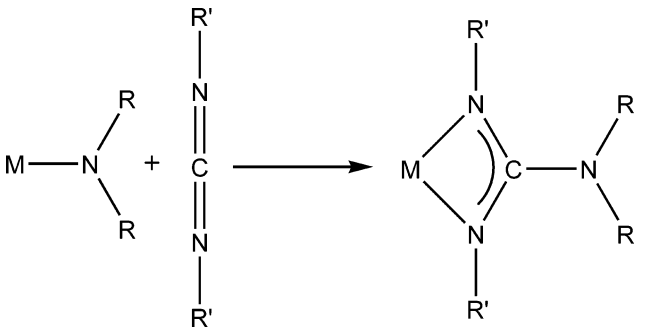

Results and Discussion

Synthesis and Spectroscopic Properties. Starting Compounds. The guanidinate ligand can be formed directly at a transition metal center by an insertion reaction of carbodiimides RN═C═NR into a metal alkyl amide bond, e.g., $L_xM\text{-}NR_2$ (Scheme 1).

In the case of tungsten, a starting material of choice would be $[(t\text{-BuN})_2W(NR'_2)_2]$ in order to yield, for example, bisguanidinato complexes of the type $[(t\text{-BuN})_2W\{(NR)_2CNR'_2\}]$. However, we failed to isolate defined and pure products along this route, presumably because of the steric bulk at the tungsten center and problems with the chemoselectivity of the insertion reaction (i.e., parallel presence of imido and amido groups). Alternatively, we investigated salt-elimination reactions, starting with octahedral $[(t\text{-BuN})_2WCl_2py_2]$ (**1**) and the lithium compounds, (TMEDA)Li[(N*i*-Pr)$_2$CN*i*-Pr$_2$] (**2a**) (TMEDA = *N*,*N*,*N*′,*N*′-tetramethyl-ethylendiamine) and $[Li(NC(NMe_2)_2)]_x$ (**2b**), as transfer reagents for the guanidinato groups (Scheme 2). The reaction of diisopropylamidolithium with one equivalent of *N*,*N*′-diisopropylcarbodiimide gives tetraisopropylguanidinatolithium, which represents a viscous gel that we could not isolate and characterize in a pure form. However, by addition of one equivalent of TMEDA, the adduct **2a** was formed in nearly quantitative yield. The compound **2a** represents a pale-yellow powder of high purity, and it was conveniently recrystallized from *n*-hexane to yield colorless to white crystals.

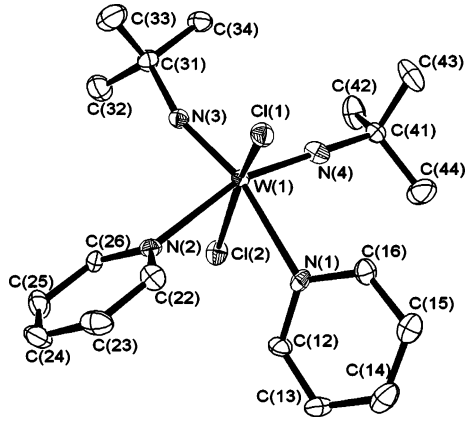

Figure 1. Molecular structure of **1** in the solid state.

The tungsten compound **1** was synthesized by a reaction scheme first reported by Becker et al.,[17] which we modified into a protocol for a one-pot synthesis (eqs 1 and 2). The ^{1}H NMR spectrum in C_6D_6 showed the expected singlet for the *t*-Bu moieties of the imido groups at 1.53 ppm and three signals with the expected intensity ratios at 6.51, 6.84, and 9.10 ppm for the pyridine ligands in accordance with the monomeric octahedral *trans*-chloro structure revealed by single-crystal X-ray diffraction, as discussed below. (Figure 1).

$$2\ WCl_6 + 8\ HN(t\text{-Bu})(SiMe_3) \rightarrow [(t\text{-BuN})_2WCl_2(NH_2t\text{-Bu})]_2 + 6\ Me_3SiCl + 2\ (t\text{-Bu})Me_3SiCl \quad (1)$$

$$[(t\text{-BuN})_2WCl_2(NH_2t\text{-Bu})]_2 + 4\ py \rightarrow 2\ [(t\text{-BuN})_2WCl_2py_2] + 2\ H_2Nt\text{-Bu} \quad (2)$$

Synthesis of [W(N*t*-Bu)$_2$Cl((N*i*-Pr)$_2$CN*i*-Pr$_2$)] (3). Treatment of **1** with **2a** in *n*-hexane and recrystallization from

Scheme 2. Synthesis of Tungsten Guanidinates

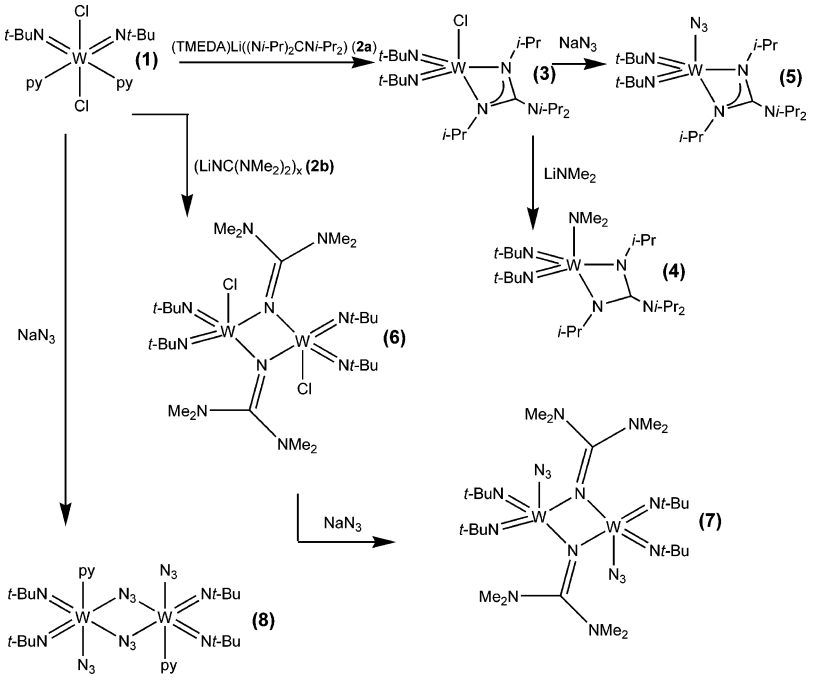

n-hexane produces bis(*tert*-butylimido)-chloro-(tetraisopropyl)guanidinato-tungsten (**3**) as yellow crystals. Attempts to substitute the remaining chloro ligand by another guanidinato group, e.g., by using an excess of **2a**, prolonged reaction times and harsher conditions (reflux) failed. The EI-MS of **3** shows the expected molecular ion peak [M^+] at m/z = 587 (8% rel int) and another peak of similar intensity at m/z = 572 that was assigned to the loss of one methyl group [$M^+ - CH_3$]. The peak at m/z = 446 (18% rel int) was attributed to a fragment ion containing the guanidinate ligand and the remaining chloro ligand bonded to the tungsten center [$M^+ - 2N$*t*-Bu]. The peak at m/z = 291 (10% rel int) was likely to relate to a protonated W−N*t*-Bu ion, resulting from a fragmented guanidinate ligand [*t*-BuNHWCl$^+$]. All peaks with $m/z \leq 226$ can be assigned to fragmentation of the guanidinato ligand, except the peak at m/z = 58 (35% rel int), which can have its origin in fragmentation of the guanidinato ligand as well as from the *t*-Bu residue at the imido ligand. The ^{1}H NMR spectrum of **3** displays one singlet for the imido groups and four different doublets for the CH_3 groups of the four isopropyl rests of the guanidinate ligand. The spectrum also reveals three septets for the CH groups, two at 4.08 and 4.15 ppm, belonging to the isopropyl groups close to the tungsten, and one at 3.17 ppm for the isopropyl groups of the amide. The doublets at 0.97 and 0.98 ppm are pointing to very similar chemical environments and are assigned to the bis-isopropylamido group N(*i*-Pr)$_2$. In addition, the rotation around the C−N(*i*-Pr)$_2$ bond axis should be slightly hindered because of steric bulk. Upon heating to 30 °C, the splitting of the two signals disappears. The asymmetric pentacoordination of the tungsten center causes the CH_3 moietes of the N*i*-Pr groups coordinated to the tungsten to be different, exhibiting resonances at 1.11 and 1.54 ppm, which remains unchanged upon heating to 60 °C. This interpretation of the NMR data referring to the molecular structure in solution at more or less ambient conditions was substantiated by the molecular structure of **3** in the solid state obtained from single-crystal X-ray diffraction studies, as discussed below (Figure 2).

Synthesis of [W(N*t*-Bu)$_2$(NMe$_2$)((N*i*-Pr)$_2$CN*i*-Pr$_2$)] (4). Aiming at an all-nitrogen coordination sphere at the tungsten center and to characterize the substitution chemistry of the remaining chloro ligand, **3** was treated with one equivalent of LiNMe$_2$ in diethyl ether. After 1 day of stirring at room temperature and workup, the substitution product bis(*tert*-butylimido)dimethylamido(tetraisopropyl)guanidinato-tungsten (**4**) was obtained as a yellow viscous oil. The EI-MS shows the molecular peak [M^+] at m/z = 596 (1% rel int). The following daughter peaks mostly show a clean cleavage of the ligands similar to those described above for compound **3**. The peaks below m/z = 226 (30% rel int.) arise only from ligand fragmentation and do not contain tungsten. The ^{1}H NMR spectrum of **4** displays an interesting feature in comparison with that of **3**. Although the signals for the *i*-Pr groups of the guanidinate ligand of **3** were splitted, the NMR spectrum of **4** does not show a splitting but only two doublets and two septets of equal intensity corresponding to only two different kinds of *i*-Pr groups. This phenomenon was also observed in the carbon NMR. Assuming a monomeric pentacoordinated structure similar to that of **3**, this situation can only be explained by a more symmetric coordination of the guanidinato ligand. In particular, a structure derived from a square pyramidal WN$_5$ arrangement with the NMe$_2$ group at the apical position and the two *t*-BuN imido groups in a cis position at the basal N$_4$ plane, likewise the two *i*-PrN groups of the guanidinato ligand, would explain the different NMR feature of **4**. This might be caused by the higher steric demand (cone angle) of the dimethylamido ligand compared to that of a chlorine atom, which forces the complex into a more symmetrical structure with equivalent environments for the *i*-PrN groups coordinated to the tungsten center. Unfortunately, we were not able to grow single crystals of **4** suitable for X-ray diffraction studies to unambiguously clarify the molecular structure of **4** in the solid state.

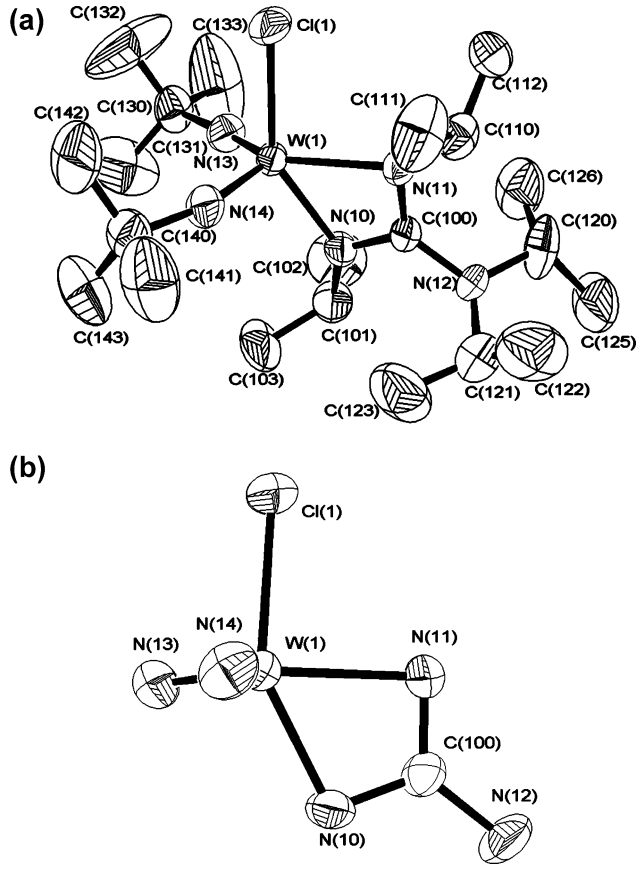

Figure 2. (a) Molecular structure of **3**. (b) Projection of the molecular Structure of **3** (*t*-Bu and *i*-Pr groups omitted for clarity) perpendicular to one of the CN$_3$ planes. According to the NMR data in solution, **4** and **5** are likely to be also monomeric and structurally closely related by the substitution of the Cl ligand against NMe$_2$ and N$_3$.

Synthesis of [W(N*t*-Bu)$_2$(N$_3$){(N*i*-Pr)$_2$CN*i*-Pr$_2$}] (5). On refluxing compound **3** in a mixture of toluene/THF together with an excess of sodium azide the complex bis(*tert*-butylimido)-azido-(tetra-*iso*-propyl)guanidinato-tungsten (**5**) was obtained as a viscous oil. **5** exhibits the characteristic, intense asymmetric ν_{as}(NN) vibration at 2086 cm^{-1} in the IR spectrum. In contrast to that of **4**, the ^{1}H NMR of **5** again exhibits the splitted signals for the *i*-PrN groups as observed for complex **3**, but with a slightly smaller difference in the chemical shift. The sterically nondemanding azido group

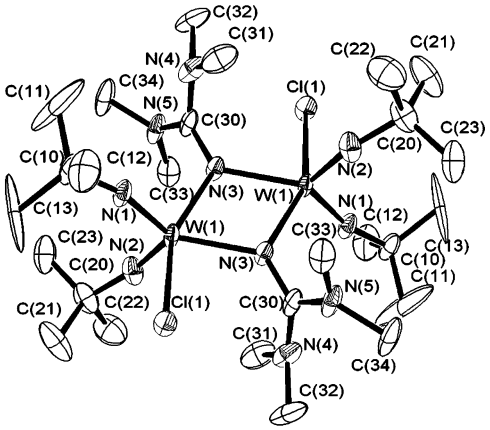

Figure 3. Molecular structure of **6** in the solid state.

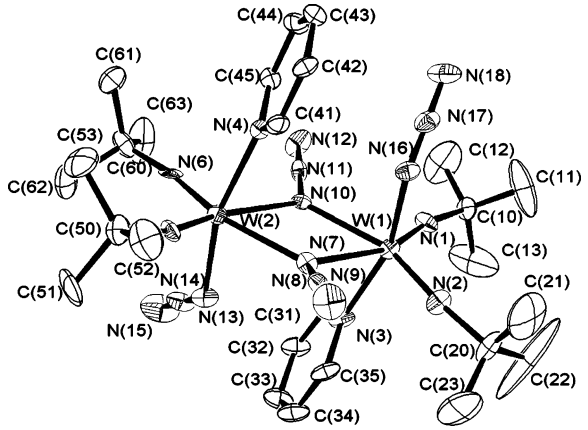

Figure 4. Molecular structure of **8**.

expectedly behaves more like the chloro than like the alkylamido ligand. We suppose that **5** again was coordinated in a distorted trigonal bipyramidal fashion rather than being derived from a more symmetric square pyramidal structure, as suggested for **4**, creating different chemical environments for the *i*-PrN groups attached to the W center. As in the case of **4** above, we failed to grow single crystals of **5** suitable for X-ray diffraction studies to unambiguously clarify the molecular structure of **5** in the solid state.

Synthesis of $[W(N\textit{t}\text{-}Bu)_2(Cl)(NC(NMe_2)_2]_2$ (6). The addition of lithiated 1,1,3,3-tetramethyl-guanidine, $[LiNC(NMe_2)_2]_x$, to **1** gives the new complex bis(bis(*tert*-butylimido)-chloro-(1,1,3,3-tetramethyl)guanidinato-tungsten) (**6**). The dimeric structure was established by single crystal X-ray diffraction studies (see below, Figure 3). In the EI-MS spectra, only the monomer was detected showing one-half of the molecular ion $[M/2^+]$ at $m/z = 475$ (1.6% rel int) and a clean fragmentation pattern of the ligands with similar features to those discussed above for the related compounds. The ^{1}H NMR reveals one signal at 1.52 ppm for the imido groups and a very broad signal for the NMe_2 groups, which might indicate a dynamic behavior of the guanidinato ligand at room temperature. The CN_3unit of the particular guanidinato−ligand requires a C−N bond with partial double-bond character. Thus, in the case of **6**, it should be possible to probe this by freezing the rotation of the ligand. For this purpose, a low-temperature ^{1}H NMR was recorded from −50 to +50 °C in steps of 10 °C. The spectrum at −50 °C shows two sharp signals at 2.39 and 3.05 ppm for each NMe_2 group of the guanidinato ligand. Upon rising the temperature, coalescence of the two signals was observed at room temperature, whereas at 45 °C one sharp singlet at 2.7 ppm was observed.

Synthesis of $[W(N\textit{t}\text{-}Bu)_2(N_3)(NC(NMe_2)_2]_2$ (7). Refluxing **6** in toluene with sodium azide leads to a chloride vs azide exchange and results in the analogous azido compound **7**. All structural details of **7** referring to the dimeric structure and the W_2N_2 ring are very similar to those of **6**, of course with the exception of the presence of the terminal azido ligand rather than a chloro group; thus the structure of **7** it is not discussed in detail here. The interested reader is asked to download the supplementary information package.

Synthesis of $[W(N\textit{t}\text{-}Bu)_2(N_3)(\mu^2\text{-}N_3)py]_2$ (8). Refluxing **1** with an excess of NaN_3 in toluene leads to the dimeric bis-(bis-*tert*-butylimido)-bisazido-pyridine tungsten **(8)**. It shows the characteristic IR absorption band at 2082 cm^{-1}. The ^{1}H NMR shows a singlet for the tungsten and pyridine signals, corresponding to one pyridine ligand per tungsten. The molecular structure of **8** in the solid state is described below (Figure 4).

Structural Chemistry of the New Complexes. The new compounds **1**, **3**, **6**, **7**, and **8** were characterized by single-crystal X-ray crystallography. Relevant crystallographic information, details on the data collection and the quality of the structure solution are compiled in Table 1. The molecular structures are depicted as Ortep drawings in Figures 1−5. Data collection and the structure solution were performed without special problems and no unusual difficulties.

Structure of $[W(N\textit{t}\text{-}Bu)_2Cl_2py_2]$ (1). Figure 1 shows the molecular structure of **1** in the solid state, revealing a tungsten center with a distorted octahedral coordination, two *trans*-chloro ligands, and cis coodinated imido and pyridine ligands, which was the typical coordination scheme for $[WCl_2(NR)_2L_x]$ ($x = 1, 2$) compounds.[20−23] The octahedral coordination can be specified by the sum of angles around the tungsten being 360.08, 356.3, and 355.5° for the three space directions.

By looking at the two W−N−C angles, one can see that both imido ligands are bonded slightly different. The W(1)−N(4)−C(41) angle is nearly linear (174.9°), whereas the other imido ligand is coordinated in a slightly bent fashion (161.3°). None of the imido ligands is in the category of strongly bent ligands (bond angle < 150°). The difference of angles might also be induced by interactions with the π systems of the pyridine ligand or by crystal-packing forces. The W−N distance to the pyridine ligand in a position trans to the linear imido group is slightly shorter than the same

(20) Bradley, D. C.; Errington, R. J.; Hursthouse, M. B.; Short, R. L.; Ashcroft, B. R.; Clark G. R.; Nielson, A. J.; Rickard, C. E. F. *J. Chem. Soc., Dalton Trans.* **1987**, 2067.
(21) Clegg, W.; Errington, R. J.; Hockless, D. C. R.; Redshaw, C. *J. Chem. Soc., Dalton Trans.* **1993**, 1965.
(22) Dreisch, K.; Andersson, C.; Stålhandske, C. *Polyhedron* **1993**, *12(11)*, 1335.
(23) Leung, W.-H.; Wu, M.-C.; Chim, J. L. C.; Wong, W.-T. *Polyhedron* **1998**, *17(4)*, 457.

Table 1. Crystallographic Data for **1**, **3**, **6**, **7**, and **8**

	1	**3**	**6**	**7**	**8**
empirical formula	$WCl_2N_4C_{18}H_{28}$	$WClN_5C_{21}H_{46}$	$W_2Cl_2N_{10}C_{26}H_{60}$	$W_2N_{16}C_{26}H_{60}$	$W_2N_{18}C_{26}H_{46}$
fw	555.19	587.93	951.44	964.60	978.51
space group	$Pna2_1$	$P\bar{1}$	$P2_1/c$	$P2_1/n$	$P\bar{1}$
a (Å)	16.4634(9)	9.059(2)	11.8101(10)	9.3581(8)	10.6021(7)
b (Å)	8.8987(4)	10.359(3)	17.1297(13)	21.4148(18)	15.9447(10)
c (Å)	14.9136(8)	15.293(4)	9.8014(6)	10.0342(9)	16.8824(10)
α (deg)	90	81.786(10)	90	90	93.330(5)
β (deg)	90	80.206(9)	109.816(7)	110.507(8)	93.330(5)
γ (deg)	90	86.217(7)	90	90	96.270(5)
V (Å^3)	2184.89(19)	1398.5(6)	1865.4(2)	1883.4(3)	2780.7(3)
Z	4	2	2	2	3
ρ_{calcd} (g cm^{-3})	1.688	1.396	1.694	1.436	1.753
μ (mm^{-1})	5.540	4.240	6.335	6.119	6.245
R1	0.0277	0.0372	0.0291	0.0510	0.0385
wR2	0.0566	0.0917	0.0728	0.0997	0.0573

Table 2. Selected Bond Lengths (Å) and Angles (deg) for **1**

W(1)−N(3)	1.761(4)	W(1)−Cl(1)	2.4150(12)
W(1)−N(4)	1.746(4)	W(1)−Cl(2)	2.4192(13)
W(1)−N(1)	2.414(4)	N(3)−C(31)	1.461(6)
W(1)−N(2)	2.396(4)	N(4)−C(41)	1.454(7)
N(4)−W(1)−N(3)	107.86(18)	N(2)−W(1)−Cl(1)	83.23(10)
N(4)−W(1)−N(2)	162.60(17)	N(1)−W(1)−Cl(1)	81.56(10)
N(3)−W(1)−N(2)	89.44(16)	N(4)−W(1)−Cl(2)	94.67(14)
N(4)−W(1)−N(1)	87.79(17)	N(3)−W(1)−Cl(2)	95.63(14)
N(3)−W(1)−N(1)	164.33(16)	N(2)−W(1)−Cl(2)	81.50(10)
N(2)−W(1)−N(1)	74.89(14)	N(1)−W(1)−Cl(2)	82.06(11)
N(4)−W(1)−Cl(1)	96.07(14)	Cl(1)−W(1)−Cl(2)	160.01(5)
N(3)−W(1)−Cl(1)	97.05(13)	C(31)−N(3)−W(1)	161.9(3)
		C(41)−N(4)−W(1)	174.9(4)

distance trans to the bent one. Also, the ligand trans to the bent imido group is twisted out of the N(1)−W(1)−N(3) plane a bit stronger than the other pyridine isout of the N(2)−W(1)−N(4) plane, which means that the less-twisted pyridine ligand trans to the linear imido group acts as a better π acceptor and thus exhibits a shorter W−N bond length.

Comparing these angles and the W−N distances of **1** with the situation of other closely related $[WCl_2(NR)_2L_x]$ compounds (Table 3), all of the other reference compounds exhibit very similar angles and bond lengths, whereas both imido ligands in **1** are bonded distinctly differently. This difference is apparently due to the presence of the chelating ligand in all of the reference compounds of Table 2. The linkage between the two pyridine groups of the bipy ligand causes a twisting of the groups to be energetically unfavorable and consequently forces the imido ligands into a more symmetric environment.

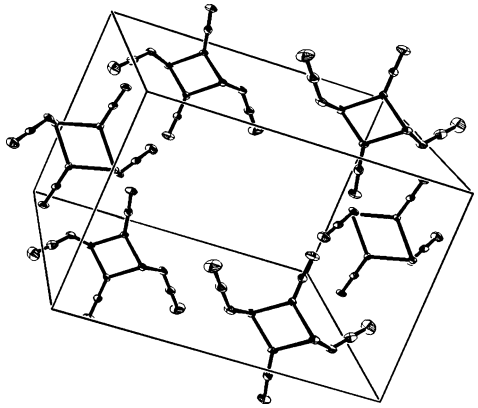

Figure 5. Different molecules of **8** in the unit cell. (Imido and pyridine ligands omitted for clarity.)

Table 3. Comparison of W═N−C Angles and W═N- Bond Lengths

	angles (deg)	bond lengths (Å)	ref
$WCl_2(Nt\text{-}Bu)_2py_2$	161.9(3)	1.761(4)	this work
	174.9(4)	1.746(4)	
$WCl_2(Nt\text{-}Bu)_2$bipy	166.4(5)	1.747(5)	21
	162.7(4)	1.754(4)	
$WCl_2(NPh)_2$bipy	165.6(12)	1.781(11)	20
	164.4(11)	1.787(14)	
$WCl_2(Nt\text{-}Bu)_2$(*t*-Bu-dab)[a]	160.8(7)	1.756(8)	23
	161.8(7)	1.758(8)	

[a] *t*-Bu-dab = *N*,*N*′-di-*tert*-butyl-1,4-diaza-1,3-butadiene.

Structure of $[W(Nt\text{-}Bu)_2Cl\{(Ni\text{-}Pr)_2CNi\text{-}Pr_2\}]$ (3). The coordination at the tungsten center of the mononuclear compound **3** (Figure 2) is described as strongly distorted trigonal bipyramidal, with the chloro ligand in the axial position and the imido groups and one of the coordinated N atoms of the guanidinato ligand in the equatorial position, with a sum of angles of 359.1° in the equatorial plane. The second N atom of the guanidinato ligand is shifted out of the ideal axial position due to its linkage to the rest of the ligand; nevertheless, the sum of angles around the tungsten in the Cl(1)−N(10)−N(11) plane is 362.3°, as expected for a trigonal bipyramidal coordination geometry. In contrast to **1**, now both imido ligands are bonded in a bent way with similar bond lengths (1.750 and 1.755 Å) and angles (163.0 and 164.2°). Weaker π interactions of the metal with the bidentate guanidinato ligand might be an explanation; also, crystal-packing forces cannot be excluded. The angle between the two imido groups (111.6°) is slightly enlarged compared to that of **1** (107.9°) due to the lower coordination number of the metal center. The W−Cl distance (2.376 Å) is slightly shorter compared to those of **1** (2.415 and 2.419 Å, respectively) again due to the lower coordination number and the missing chorine atom in the trans position competing for electron density. As a consequence of the steric demand of the isopropyl group at N(12), the whole amide group is twisted out of the N(10)−C(100)−N(11) plane, possibly resulting in a reduced conjugation of the lone pair at N(12) with the delocalized π system of the guanidinate ligand. The isopropyl groups at N(10) and N(11), close to the tungsten, are positioned in different chemical environments, which was already confirmed by ^{1}H NMR studies. The first one, bonded to the equatorial N(11) atom, is close to the apical chloro ligand, whereas the other one, bonded to the axial N(10)

Table 4. Selected Bond Lengths (Å) and Angles (deg) for **3**

W(1)−Cl(1)	2.3760(16)	N(13)−C(130)	1.461(7)
W(1)−N(10)	2.089(5)	N(14)−C(140)	1.429(9)
W(1)−N(11)	2.215(4)	N(10)−C(100)	1.338(7)
W(1)−N(13)	1.750(5)	N(11)−C(100)	1.307(7)
W(1)−N(14)	1.755(5)	N(12)−C(100)	1.414(7)
N(13)−W(1)−N(10)	100.4(2)	W(1)−N(10)−C(100)	96.5(3)
N(13)−W(1)−N(11)	135.0(2)	W(1)−N(11)−C(100)	91.7(3)
N(13)−W(1)−N(14)	117.7(2)	W(1)−N(13)−C(130)	164.2(5)
N(13)−W(1)−Cl(1)	94.62(17)	W(1)−N(14)−C(140)	163.0(5)
N(10)−W(1)−N(11)	60.58(17)	N(10)−C(100)−N(11)	110.6(5)
N(10)−W(1)−N(14)	103.7(2)	N(10)−C(100)−N(12)	121.5(5)
N(10)−W(1)−Cl(1)	14.93(14)	N(11)−C(100)−N(12)	127.9(5)
N(11)−W(1)−N(14)	112.3(2)		

Table 5. Selected Bond Lengths (Å) and Angles (deg) for **6**

W(1)−Cl(1)	2.4509(10)	N(2)−C(20)	1.463(6)
W(1)−N(1)	1.753(4)	N(3)−C(30)	1.328(5)
W(1)−N(2)	1.757(4)	C(30)−N(4)	1.334(7)
W(1)−N(3)	2.059(3)	C(30)−N(5)	1.367(6)
N(1)−C(10)	1.450(5)		
N(1)−W(1)−N(2)	110.54(18)	W(1)−N(3)−C(30)	122.8(3)
N(1)−W(1)−N(3)	98.42(15)	N(3)−C(30)−N(4)	123.6(4)
N(1)−W(1)−Cl(1)	90.52(11)	N(3)−C(30)−N(5)	119.8(5)
N(2)−W(1)−N(3)	106.79(15)	N(4)−C(30)−N(5)	116.6(4)
N(2)−W(1)−Cl(1)	94.44(12)	C(30)−N(4)−C(31)	119.5(4)
N(3)−W(1)−Cl(1)	152.13(10)	C(30)−N(4)−C(32)	121.6(4)
W(1)−N(1)−C(10)	166.0(3)	C(30)−N(5)−C(33)	119.8(4)
W(1)−N(2)−C(20)	159.0(3)	C(30)−N(5)−C(34)	122.1(4)

atom, is positioned toward the imido ligands. The symmetry of the "free" CN_3 moiety is somewhat distorted by the coordination to the tungsten center with a bite angle N(10)−C(100)−N(11) of 110.6°, but the CN_3 system it is still strictly planar ($\sum$ angles = 359.1°) (see Table 4).

Structure of [W(N*t*-Bu)$_2$(Cl)(NC(NMe$_2$)]$_2$ (6). The molecule structure of **6** (Figure 3) shows a dimeric species with the μ^2-bonded guanidinato ligands {NC(NMe$_2$)$_2$}. The coordination sphere of the tungsten atoms is best described as two distorted trigonal bipyramids linked over the edges, where the angles around the tungsten in the N(1)−N(2)−N(3) plane add to 359.8°. Perpendicular to that, within the plane defined by Cl(1) and the bridging nitrogen atoms, the sum of angles is 362.4°. The angle of 110.5° between the two equatorial *t*-BuN imido groups is quite similar to the situation observed for the mononuclear compound **3**. The CN_3 unit of the guanidinato ligands is nearly perfectly trigonal planar, with all N−C−N angles near 120° and a sum of angles around C(30) of exactly 360°. Also, all other bond angles in the guanidinato ligand, including the W(1)−N(3)−C(30) angle, are close to 120° (see Table 5). The sp^2 hybridization of the atoms enables the lone pairs of the N atoms to effectively donate electron density toward the tungsten. The comparably short C−N bond distances also indicate the delocalized CN multiple bond character in the CN_3 unit. The observed twisting of the guanidinato ligands toward the W(1)−N(3)−W(1) plane is likely to reduce the electron donation of the dimethylamido groups toward the tungsten center. However, the temperature-dependent ^{1}H NMR showed a hindered rotation of the ligand, pointing to the issue of electron-density donation to the tungsten center. This dynamic situation finally allows a formal configuration of 18 valence electrons for each tungsten.

Table 6. Selected Bond Lengths (Å) and Angles (deg) for **8**

W(1)−N(1)	1.759(5)	N(1)−C(10)	1.454(7)
W(1)−N(2)	1.749(5)	N(2)−C(20)	1.467(7)
W(1)−N(3)	2.200(5)	N(7)−N(8)	1.235(6)
W(1)−N(7)	2.312(5)	N(8)−N(9)	1.142(6)
W(1)−N(10)	2.285(5)	N(16)−N(17)	1.207(6)
W(1)−N(16)	2.090(5)	N(17)−N(18)	1.154(6)
N(1)−W(1)−N(2)	108.0(2)	N(7)−W(1)−N(10)	65.04(15)
N(1)−W(1)−N(3)	94.59(19)	N(7)−W(1)−N(16)	81.54(18)
N(1)−W(1)−N(7)	158.3(2)	N(10)−W(1)−N(16)	86.95(18)
N(1)−W(1)−N(10)	93.35(19)	W(1)−N(1)−C(10)	166.9(4)
N(1)−W(1)−N(16)	97.2(2)	W(1)−N(2)−C(20)	169.1(4)
N(2)−W(1)−N(3)	92.89(19)	W(1)−N(7)−N(8)	118.0(4)
N(2)−W(1)−N(7)	93.7(2)	W(1)−N(10)−N(11)	122.7(4)
N(2)−W(1)−N(10)	157.5(2)	W(1)−N(16)−N(17)	125.8(4)
N(2)−W(1)−N(16)	97.1(2)	N(7)−N(8)−N(9)	179.0(6)
N(3)−W(1)−N(7)	82.13(17)	N(10)−N(11)−N(12)	178.2(6)
N(3)−W(1)−N(10)	78.00(17)	N(16)−N(17)−N(18)	175.9(6)
N(3)−W(1)−N(16)	161.4(2)		

Table 7. Comparison of W−N Distances in [W(N*t*-Bu)$_2$N$_3$$\mu^2$-N$_3$L]$_2$

	L = py	L = *t*-BuNH$_2$
W−azide	2.090(5)	2.156(14)
W−μ^2azide	2.285(5)	2.357(16)
W−L	2.200(5)	2.185(14)
W−imide	1.749(5)	1.734(16)
	1.759(5)	1.794(15)

Structure of [W(N*t*-Bu)$_2$(N$_3$)(μ^2-N$_3$)py]$_2$ (8). The molecular structure (Figure 4) reveals a dinuclear complex with two tungsten atoms now resting in a distorted octahedral environment, as indicated by the sum of angles around W(1) being 360.2, 355.5, and 354.9° for all three directions (see Table 6). These two WN_6 octahedrons are linked together in an edge-sharing mode. Two azido ligands are in bridging positions (typical head-bridging mode of azido ligands), whereas two other azido moieties are located terminally and η^1-bonded. Comparing the W−N distances in **8** with the analogous distances in the closely related known complex [W(N*t*-Bu)$_2$(N$_3$)(μ^2-N$_3$)(*t*-BuNH$_2$)]$_2$ [24](Table 7), the new compound **8** reveals somewhat more strongly bonded azido ligands, possibly due to the pyridine ligand which is a stronger π donor than the primary amine, and thus, back-donation effects may be increased, which causes shorter W−N$_{azide}$ bonds. Also, the pyridine ligands of **8** appear to be a bit more strongly bonded compared to those of **1**. The W−N distance (2.20 Å) is significantly shorter than those found for **1** (2.396 and 2.414 Å, respectively), which is correspondingly attributed to the azido group in the trans position being clearly a much stronger π acceptor than a chloro ligand. The bond angles between the imido groups of **8** (angle N(1)−W(1)−N(2) = 107.98°) are identical with those found for the parent compound **1** (107.86°). A significant widening of that angle, similar to those of **3**, **6**, and **7**, is not observed, which is most likely due to the higher coordination number of **8**.

8 is one of the very few examples that has three crystallographic independent molecules per unit cell. In each of these, the η^1-bonded azides are orientated differently so that the unit cell contains different chiral forms of the

(24) Lam H.-W.; Wilkinson G.; Hussain-Bates, B.; Hursthouse, M. B. *J. Chem. Soc., Dalton Trans.* **1993**, 781.

complex (Figure 5). This situation is interesting for its own merit from a crystallographic and structural point of view. However, a complete and detailed discussion is beyond the scope of this article here, and the reader is asked to download the CIF files and plots from the Supporting Information.

Conclusions

We have described a series of new tungsten(VI)guanidinato complexes focusing on all nitrogen-coordination spheres of the type WN_5 and WN_6. The compound [W(N*t*-Bu)$_2$Cl$_2$py$_2$] (**1**) was found to be a very good starting material for the introduction of guanidinato ligands at tungsten(VI). The presumably mononuclear, monomeric pentacoordinated all-nitrogen complexes [W(N*t*-Bu)$_2$(NMe$_2$)((N*i*-Pr)$_2$CN*i*-Pr$_2$)] (**4**) and [W(N$_3$)(N*t*-Bu)$_2${(N*i*-Pr)$_2$CN*i*-Pr$_2$}] (**5**) seem to be particularly interesting as candidates for subsequent studies aiming at deposition of WN_x and WN_xC_y phases and thin film materials by metal-organic chemical vapor deposition techniques (MOCVD), as has been described for related transition metal guanidinato compounds of tantalum and titanium as well as recently hafnium.[13,14,25] The key compounds for WN_x MOCVD still are the bisimido−bisamido precursors of the type [(RN)$_2$W(NR′$_2$)$_2$], which find application in MOCVD and atomic layer deposition (ALD).[17] Our work suggests that a substitution of the amide ligands at the bis-*tert*-butylimido fragment [(*t*-BuN)$_2$W] by guanidinates and other nitrogen-containing ligands, in particular azido groups, opens novel possibilities of tuning the system for special applications. In particular, the azido derivative **5**, [W(N$_3$)(N*t*-Bu)$_2${(N*i*-Pr)$_2$CN*i*-Pr$_2$}], can repeatedly be sublimed at 80 °C, 1 Pa without change. We suggest **5** as an interesting precursor for WN_x deposition, especially by photoassisted methods because of the presence of the photolabile azido group as the tailored breaking point of the molecule. Similarly, the guanidinato ligand-free bis-azido complex [W(N*t*-Bu)$_2$(N$_3$)(μ^2-N$_3$)py]$_2$ (**8**) may hold promise as an entry into the chemistry of bis-imido tungsten(IV) complexes by photoreduction, ideally releasing the two azido groups in the form N_2. However, organic azides are well-known to produce nitrenes by photolytic denitrogenation, which causes a variety of subsequent insertion reactions.[26−29] A detailed study of the photochemistry of **5** and **8** is underway. We have investigated the *thermal* decomposition of related bis-azido precursors for metal nitrides in much detail choosing MOCVD of GaN from compounds of the type (N$_3$)$_2$GaR (R = (CH$_2$)$_3$NMe$_2$) and other alkyl ligands capable of intramolecular adduct formation as examples.[30] The high-temperature species GaN_3 was found to be the key intermediate of the decomposition of the molecule and the important species for GaN thin film growth.[31] We suggest that a close investigation of our mixed azido/imido/guanidinato complexes holds much promise along these lines outlined above.

Acknowledgment. Financial support by the German Research Foundation (Priority Program 1119) is gratefully acknowledged. A.B. thanks the Fonds der Chemischen Industrie (FCI) for a stipend.

Supporting Information Available: X-ray crystallographic data in CIF format for the structures of **1**, **3**, **6**, **7**, and **8**. This material is available free of charge via the Internet at http://acs.pubs.org.

IC0512431

(25) Milanov A. Master Thesis, Ruhr-Universität Bochum, Bochum, Germany, 2005.

(26) Harmer, M. A. *Langmuir* **1991**, *7(10)*, 2010.
(27) Li, Y.-Z.; Kirby, J. P.; George, M. W.; Poliakoff, M.; Schuster, G. B. *J. Am. Chem. Soc.* **1988**, *110*, 8092.
(28) Formentín, P.; Álvaro, M.; García, H.; Palomares, E.; Sabater, M. J. *New J. Chem.* **2002**, *26*, 1646.
(29) Hayashi, K.; Kanayama, T.; Shimizu, T.; Kawamura, Y.; Kameko, K.; Kawakita, S. *J. Vac. Sci. Technol., A* **2002**, *20(3)*, 995.
(30) Parala, H.; Devi, A.; Wohlfahrt, A.; Winter, M.; Fischer, R. A. *Adv. Funct. Mater.* **2001**, *11(3)*, 224.
(31) Mueller, J.; Bendix, S. *Chem. Commun.* **2001**, 911.